Accepted Manuscript


# Spectral, thermal and kinetic studies of charge-transfer complexes formed between the highly effective antibiotic drug metronidazole and two types of acceptors: σ- and π-acceptors

Moamen S. Refat, Hosam A. Saad, Abdel Majid A. Adam

PII: S1386-1425(15)00039-6
DOI: http://dx.doi.org/10.1016/j.saa.2015.01.029
Reference: SAA 13197

To appear in: *Spectrochimica Acta Part A: Molecular and Biomolecular Spectroscopy*

Received Date: 4 November 2014
Revised Date: 8 January 2015
Accepted Date: 15 January 2015

Please cite this article as: M.S. Refat, H.A. Saad, A.M.A. Adam, Spectral, thermal and kinetic studies of charge-transfer complexes formed between the highly effective antibiotic drug metronidazole and two types of acceptors: σ- and π-acceptors, *Spectrochimica Acta Part A: Molecular and Biomolecular Spectroscopy* (2015), doi: http://dx.doi.org/10.1016/j.saa.2015.01.029

This is a PDF file of an unedited manuscript that has been accepted for publication. As a service to our customers we are providing this early version of the manuscript. The manuscript will undergo copyediting, typesetting, and review of the resulting proof before it is published in its final form. Please note that during the production process errors may be discovered which could affect the content, and all legal disclaimers that apply to the journal pertain.

ACCEPTED MANUSCRIPT

# Spectral, thermal and kinetic studies of charge-transfer complexes formed between the highly effective antibiotic drug metronidazole and two types of acceptors: σ- and π-acceptors

Moamen S. Refat[a,b,*], Hosam A. Saad[a,c] and Abdel Majid A. Adam[a]

[a] *Department of Chemistry, Faculty of Science, Taif University, Al-Haweiah, P.O. Box 888, Zip Code 21974, Taif, Saudi Arabia*
[b] *Department of Chemistry, Faculty of Science, Port Said University, Port Said, Egypt*
[c] *Department of Chemistry, Faculty of Science, Zagazig University, Zagazig, Egypt*

**Abstract**

Understanding the interaction between drugs and small inorganic or organic molecules is critical in being able to interpret the drug-receptor interactions and acting mechanism of these drugs. A combined solution and solid state study was performed to describe the complexation chemistry of drug metronidazole (MZ) which has a broad-spectrum antibacterial activity with two types of acceptors. The acceptors include, σ-acceptor (i.e., iodine) and π-acceptors (i.e., dichlorodicyanobenzoquinone (DDQ), chloranil (CHL) and picric acid (PA)). The molecular structure, spectroscopic characteristics, the binding modes as well as the thermal stability were deduced from IR, UV-vis, $^{1}$H NMR and thermal studies. The binding ratio of complexation (MZ: acceptor) was determined to be 1:2 for the iodine acceptor and 1:1 for the DDQ, CHL or PA acceptor, according to the CHN elemental analyses and spectrophotometric titrations. It has been found that the complexation with CHL and PA acceptors increases the values of enthalpy and entropy, while the complexation with DDQ and iodine acceptors decreases the values of these parameters compared with the free MZ donor.

**Keywords:** Metronidazole, Charge-transfer complex, σ-acceptor, π-acceptor, TG and DTG.

* Corresponding author.
*E-mail address*: msrefat@yahoo.com (M.S. Refat).
Tel.: 00966551352497

ACCEPTED MANUSCRIPT

## 1. Introduction

The study of the charge-transfer (CT) or proton-transfer interaction of drugs and small molecularly acceptors have been a great deal of interest. It is a relevant topic in life science, pharmacology, chemistry, and medicine. During the last decade, a large number of studies have been reported on drug-acceptor interaction in solid state and in solution. The drug-acceptor complexation is an important technique that is cheaper, simpler, and more efficient than the methods of drug determination described in the literature. Also, the study of this complexation may be useful in understanding the drug-receptor interactions and the mechanism of drug action. Furthermore, the crystalline drug-acceptor complexes have a vital role in biological systems such as antimicrobial activity and DNA-binding. Literature shows that these complexes exhibit potential antimicrobial properties against some Gram-positive and Gram-negative bacteria as well as fungi [1-10]. Nitroimidazole derivatives have showed broad varieties of biological activities especially antimicrobial activity. 5-nitroimidazole based drugs have been applied to treat the infections induced by bacteria and a range of pathogenic protozoan parasites for many years because nitroimidazole derivatives can undergo bioreduction to produce electrophilic substances that can damage portion and nucleic acids [11]. In this work, the drug-acceptor interaction between drug metronidazole (MZ) and some σ- and π-acceptors was reported. The acceptors include, σ-acceptor (i.e., iodine) and π-acceptors (i.e., dichlorodicyanobenzoquinone (DDQ), chloranil (CHL) and picric acid (PA)). Metronidazole (MZ; $C_6H_9N_3O_3$) chemically 1-(2-hydroxyethyl)-2-methyl-5-nitroimidazole, the structure of which is shown in Scheme 1, is a 5-nitroimidazole-based drug with highly antibiotic and anticoccidial activity [12]. It is an antibiotic used to treat different kinds of infections and frequently used in treating anaerobic and protozoal infections [13-15]. MZ is used in surgery, especially breast cancer and colon cancer surgery [16], and as a promoter to induce the growth of cattle, pigs, and poultry and improve feed efficiency [17]. It is generally well tolerated, although it has been banned by many countries and areas from use in food producing animals because MZ is now believed to possess genotoxic, carcinogenic and mutagenic side effects. MZ binds to DNA causing its damage; on the other hand it is capable of inducing gene mutations in mammalian cells. It may be carcinogenic in mice and rates if used in large doses for an extended period of time [18-20]. The objectives of the current study were as follows: *(i)* to synthesize the CT complexes of drug MZ with iodine, DDQ, CHL and PA acceptors; *(ii)* to characterize the formed complexes structurally via infrared (IR), $^1$H NMR, and electronic absorption spectroscopy; *(iii)* to observe and differentiate the thermal behavior of the reported complexes using TG and DTG techniques.

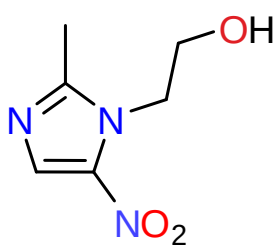


**Scheme 1.** Chemical structure of drug metronidazole (MZ).

ACCEPTED MANUSCRIPT

## 2. Experimental methodologies

### *2.1 Reagents and solutions*

Drug metronidazole (MZ; $C_6H_9N_3O_3$; 171.15) was obtained from Sigma-Aldrich Chemical Company (USA) with a stated purity of greater than 98% and it was used as such without further purification. The electron acceptors iodine ($I_2$; 253.8), 2,3-dichloro-5,6-dicyano-1,4-benzoquinone (DDQ; $C_8Cl_2N_2O_2$; 227), chloranil (CHL; $C_6Cl_4O_2$; 245.88) or picric acid (PA; $C_6H_3N_3O_7$; 229.10) (Scheme 2) and other spectroscopic grade solvents were purchased from Aldrich and Merck Chemical Companies and were used without modification. All chemicals used in this study were of analytical reagent grade and used without further purification. A standard stock solutions of MZ and each acceptor at a concentration of $5.0\times10^{-3}$ M were freshly prepared prior to each series of measurements by dissolving precisely weighed quantities in a 100 mL volumetric flask using methanol or chloroform solvent. The stock solutions of MZ and acceptors were protected from light. Solutions for spectroscopic measurements were made by mixing appropriate volumes of donor and acceptor stock solutions with the solvent immediately before running the spectra.

### *2.2 Reaction chemistry*

To obtain the CT complexes, a methanol or chloroform solution of MZ (1 mmol) was stirred with a solution of each acceptor (1 mmol) in the same solvent for *ca*. 30 min on a magnetic stirrer at room temperature. A change in color developed, and the volume of the solution was reduced to one-half by evaporation on a water bath, resulting in the precipitation of the solid CT complexes. The formed complexes were isolated, filtered off and washed twice thoroughly with the minimum given solvent to obtain the pure products. The solid products were then collected and dried *in vacuo* for 48 h. Strong change in colors was observed upon mixing solutions of the MZ donor with any of the acceptors. These observed new colors are dark brown for MZ–$I_2$ and MZ–CHL, dark-reddish brown for MZ–DDQ and dark yellow for MZ–PA reaction mixtures. These changes in colors represent strong evidence of the CT interactions between the donor and each of the acceptors. These complexes were characterized by spectroscopy (IR, $^1$H NMR and UV-vis) elemental and thermal analysis.

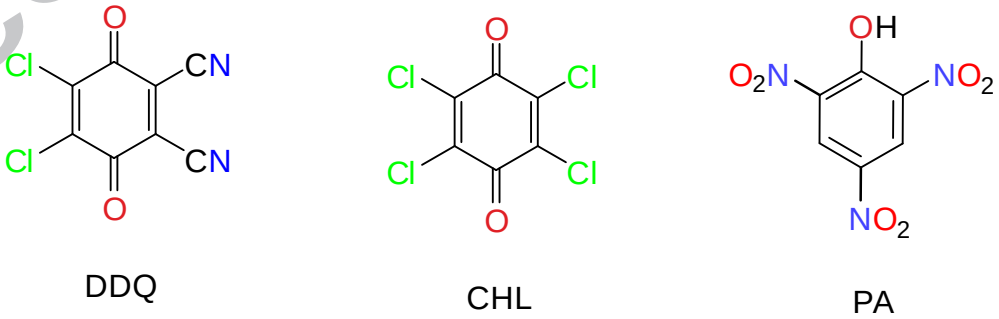


**Scheme 2.** Chemical structure of the DDQ, CHL and PA acceptors.

ACCEPTED MANUSCRIPT

*2.3 Experimental measurements*

To determine the stoichiometry of the MZ–acceptor interactions, various molar ratio were examined by spectrophotometric titration measurements. These titrations monitored the detectable CT bands during the reactions of $I_2$, DDQ, CHL or PA with MZ. Briefly, 0.25, 0.50, 0.75, 1.00, 1.50, 2.0, 2.50, 3.00, 3.50 or 4.00 mL of a standard solution ($5.0\times10^{-4}$ M) of the appropriate acceptor in methanol or chloroform solvent was added to 1.00 ml of the MZ donor at $5.0\times10^{-4}$ M, dissolved in the same solvent. The final volume of the mixture was 5 ml. The concentration of the donor ($C_d$) was maintained at $5.0\times10^{-4}$ M, whereas the concentration of the acceptor ($C_a$) varied from $0.25\times10^{-4}$ M to $4.00\times10^{-4}$ M to produce solutions with a (donor: acceptor) molar ratio that varied from 4:1 to 1:4. The absorbance of each complex was plotted against the volume of the added acceptor.

*2.4 Calculations background*

*2.4.1 Spectroscopic data*

In the solution state, the spectroscopic data of the formed CT complexes were calculated as summarized below. The formation constant ($K$) and the molar extinction coefficient ($\varepsilon$) were determined spectrophotometrically using the 1:1 Benesi–Hildebrand equation (Eq. 1) [21] for the (1:1) CT complexes (with DDQ, CHL and PA acceptors) or the 1:2 modified Benesi–Hildebrand equation (Eq. 2) [22] for the (1:2) CT complexes (with iodine acceptor). $C_a$ and $C_d$ are the initial concentrations of the acceptor and donor, respectively, and $A$ is the absorbance of the CT band. By plotting the $(C_aC_d)/A$ values for the 1:1 CT complex as a function of the corresponding $(C_a+C_d)$ values or $(C_a)^2C_d/A$ values against $C_a(4C_d+C_a)$ values for the 1:2 CT complex, a straight line is obtained with a slope of $1/\varepsilon$ and an intercept at $1/K\varepsilon$. The values of energy ($E_{CT}$) of the interactions, oscillator strength ($f$), transition dipole moments ($\mu$) and standard free energy change ($\Delta G°$) were calculated as described elsewhere [23-26].

$$(C_aC_d)/A = 1/K\varepsilon + (C_a + C_d)/\varepsilon \quad (1)$$

$$(C_a)^2C_d/A = 1/K\varepsilon + 1/\varepsilon\, C_a\,(4C_d + C_a) \quad (2)$$

*2.4.2 Kinetic–thermodynamic data*

Two methods were used to evaluate the kinetic–thermodynamic parameters; the Coats–Redfern method [27] and the Horowitz–Metzger [28] method. The Coats–Redfern equation, which is an atypical integral method, can be represented using (Eq. 3). $\alpha$ is the fraction of the sample decomposed at time $t$, $T$ is the derivative peak temperature, $A$ is the frequency factor, $R$ is the gas constant, $E^*$ is the activation energy, and $\varphi$ is the linear heating rate. A plot of the left-hand side (LHS) against $1/T$ was constructed. $E^*$ is the activation energy in kJ mol$^{-1}$ and was calculated from the slope. The $A$ (s$^{-1}$) value was calculated from the intercept. The Horowitz–Metzger equation can be represented using (Eq. 4). $\theta = T - T_s$, $w_\gamma = w_\alpha - w$, $w_\alpha$ is the mass loss at the completion of the reaction, and $w$ is the mass loss at time $t$. The plot of Log [log $(w_\alpha/w_\gamma)$] versus $\theta$ was constructed and was observed to be linear, and $E^*$ was calculated from its slope.

$$\mathrm{Ln}[-\ln(1-\alpha)/T^2] = -E^*/RT + \ln[AR/\varphi E^*] \quad (3)$$

$$\mathrm{Log}\,[\log(w_\alpha/w_\gamma)] = E^*\theta/2.303RT_s^2 - \log 2.303 \quad (4)$$

ACCEPTED MANUSCRIPT

*2.5 Equipments*

Elemental analyses for the C, H and N contents of the solid compounds were performed by the microanalysis facility at Cairo University, Egypt, using a Perkin–Elmer CHN 2400 (USA). All of the electronic absorption spectral measurements were recorded in methanol or chloroform over a wavelength range of 200–800 nm using a Perkin–Elmer Lambda 25 UV/Vis double-beam spectrophotometer at Taif University, Saudi Arabia. The instrument was fitted with a quartz cell with a path length of 1.0 cm. The infrared (IR) spectra of the solid CT complexes (as KBr discs) were acquired at room temperature using a Shimadzu FT-IR spectrophotometer instrument (Japan) in the range of 4000–400 $cm^{-1}$ for 30 scans at a 2 $cm^{-1}$ resolution. The Raman laser spectra were performed on a Bruker FT-Raman spectrophotometer equipped with a 50 mW laser. The NMR spectra were recorded on Varian Mercury VX-300 NMR spectrometer. $^{1}H$ spectra were run at 300 MHz in dimethylsulphoxide (DMSO-d6). Chemical shifts are quoted in δ and were related to that of the solvents. The measurements were performed at ambient temperature using DMSO-$d_6$ (dimethylsulfoxide, $d_6$) as a solvent and TMS (tetramethylsilane) as an internal reference. The $^{1}H$ NMR data are expressed in parts per million (ppm) and are internally referenced to the residual proton impurity in the DMSO solvent. Thermogravimetric analyses (TG and DTG) was performed under nitrogen atmosphere between room temperature and 800 °C at a heating rate of 10 °C/min using a Shimadzu TGA–50H thermal analyzer at the Central Lab at Cairo University, Egypt.

## 3. Results and discussion

*3.1 Elemental analysis results*

The synthesized solid complexes were analyzed in terms of their carbon, hydrogen, and nitrogen content in order to determine the stoichiometry of the complex formation. The elemental analyses data were in satisfactory agreement with the calculated values. The results of the formed CT complexes are as follows. (MZ–$I_2$): $C_6H_9N_3O_3I_4$; Mol. wt. = 678.75; Calc.: %C, 10.61; %H, 1.33; %N, 6.19, Found: %C, 10.57; %H, 1.30; %N, 6.15. (MZ–DDQ): $C_{14}H_9Cl_2N_5O_5$; Mol. wt. = 398.16; Calc.: %C, 42.23; %H, 2.28; %N, 17.59, Found: %C, 42.19; %H, 2.25; %N, 17.62. (MZ–CHL): $C_{12}H_9Cl_4N_3O_5$; Mol. wt. = 417.04; Calc.: %C, 34.53; %H, 2.16; %N, 10.07, Found: %C, 34.50; %H, 2.12; %N, 10.11. (MZ–PA): $C_{12}H_{12}N_6O_{10}$; Mol. wt. = 400.26; Calc.: %C, 36.01; %H, 3.02; %N, 21.0, Found: %C, 36.06; %H, 2.97; %N, 21.1. The stoichiometry of the interaction between the MZ donor and the acceptors was found to be 1:2 for the iodine acceptor and 1:1 for the DDQ, CHL and PA acceptors.

*3.2 Characteristics CT bands*

Figure 1 displays the electronic absorption spectra of the MZ donor ($5.0\times10^{-4}$ M) and the acceptor ($5.0\times10^{-4}$), along with those of the prepared CT complexes for the MZ–$I_2$, MZ–DDQ, MZ–CHL, MZ–PA systems, respectively. These figures indicated change in the UV-Vis spectrum of the donor upon the addition of the acceptor and revealed the presence of the absorption bands that correspond to the CT interactions. The absorption bands appeared at 280 and 365 for $I_2$ complex, 400 and 525 for DDQ complex, 217 for CHL complex and 370 nm for PA complex, respectively, are presumably due to the MZ–acceptor interactions and are indicative of the formation of a CT complex. The MZ donor displays a strong band at 230 nm.

ACCEPTED MANUSCRIPT

On mixing the solutions of the donor and acceptors, this characteristic band red-shifts, increases strongly in intensity in $I_2$ complex, while it blue-shifts, increases strongly in intensity and becomes more broad in CHL and PA complexes. This band is centered at 237, 230, 217 and 215 nm for MZ–$I_2$, MZ–DDQ, MZ–CHL and MZ–PA products, respectively. The spectrum of the MZ–$I_2$ complex was characterized by two significant broad bands at 280 and 365 nm that correspond to the MZ–iodine interaction. The appearance of these two bands is well known to be characteristic of the formation of the triiodine ion ($I_3^-$) [29-31]. The observed electronic absorption spectrum of the iodine complex confirmed the formation of the $[MZ–I]^+I_3^-$ complex. The absorption spectrum of the formed DDQ complex revealed the presence of a new broad band observed in the visible region (at 525 nm). Neither free MZ donor nor free DDQ acceptor has measurable absorptions at this wavelength. This new broad band at longer wavelength is indicative of the formation of the CT complex between MZ and DDQ.

*3.3. Stoichiometry of the interaction*

The stoichiometry of the formed CT complexes between the MZ donor and the acceptors was determined by applying a varying molar ratio spectrophotometric titration method. The electronic spectra of the MZ–acceptor systems were recorded with varying concentrations of acceptor and a constant MZ concentration. The composition of the complexes was determined graphically by plotting the absorbance as a function of the volume of acceptor (in mL). Representative spectrophotometric titration plots based on the characterized absorption bands are shown in Figure 2. The results show that the largest interaction between MZ donor and each acceptor occurred at a MZ: acceptor ratio of 1:2 for iodine acceptor and of 1:1 for DDQ, CHL and PA acceptors. The structures of the new formed CT complexes were formulated to be $[MZ–I]^+I_3^-$, [(MZ)(DDQ)], [(MZ)(CHL)] and [(MZ)(PA)]. These structures and stoichiometries agree quite well with the elemental analyses of the formed solid complexes.

*3.4 Spectroscopic data*

Representative Benesi–Hildebrand plots are shown in Figure 3, and the values of both $K$ and $\varepsilon$ are thus determined and are given in Table 1 along with the other spectroscopic data ($f$, $\mu$, $E_{CT}$ and $\Delta G°$) calculated as previously described in section (2.4.1). In general, the 1:2 complexes exhibit high values for the formation constants ($K$). The MZ–$I_2$ complex shows higher $K$ value compared with the other 1:1 complexes. This high $K$ value indicates a strong interaction between the MZ–$I_2$ pairs and confirms a high stability of the prepared complex. The complex stability is strongly dependent on the nature of the used acceptor including the type of electron withdrawing subsitituents to it such as nitro and halo groups. The complex containing the DDQ acceptor exhibits a higher $K$ value compared with the other 1:1 complexes, which reflects the relatively higher powerful electron acceptance ability of DDQ. The DDQ acceptor has two cyano and two chloro groups between two carbonyl groups. This causes high delocalization leads to a great increase in the Lewis acidity of the acceptor, and hence the higher value of $K$ for its complex compared with the others. The observed high value of $K$ suggests that the formed CT complex is strongly bound and highly stable. The stability of the 1:1 complexes decreases in the following order: MZ–DDQ > MZ–PA > MZ–CHL. The MZ–DDQ complex also exhibits higher values of both $f$ and $\mu$, which indicates a strong interaction between the MZ–DDQ

ACCEPTED MANUSCRIPT

pairs with relatively high probabilities of CT transitions. All of the $\Delta G°$ values are negative. These negative values indicate that the interaction between the MZ donor and the acceptors is spontaneous. The $\Delta G°$ values of the complexes in decreasing order for the different acceptors are as follows: $I_2$ > DDQ > PA > PA.

**Table 1.** Spectral properties of the MZ–acceptor CT complexes at 298 K.

| Property | Complexes | | | |
|---|---|---|---|---|
| | MZ–$I_2$ | MZ–DDQ | MZ–CHL | MZ–PA |
| $\lambda_{max}$ (nm) | 280 | 525 | 217 | 370 |
| Formation constant; $K$ ($Lmol^{-1}$) | $5.25\times10^{7}$ | $10.64\times10^{4}$ | $7.22\times10^{4}$ | $9.83\times10^{4}$ |
| Extinction coefficient; $\varepsilon_{max}$ ($Lmol^{-1}cm^{-1}$) | $123\times10^{4}$ | $13.6\times10^{4}$ | $2.88\times10^{4}$ | $12.9\times10^{4}$ |
| Energy value; $E_{CT}$ (eV) | 4.44 | 2.37 | 5.73 | 3.36 |
| Oscillator strength; $f$ | 17.72 | 9.82 | 2.74 | 7.26 |
| Dipole moment; $\mu$ | 32.47 | 10.47 | 3.56 | 6.99 |
| Free energy; $\Delta G^{o}$ (kJ $mol^{-1}$) | $-4.41\times10^{4}$ | $-3.44\times10^{4}$ | $-3.40\times10^{4}$ | $-3.42\times10^{4}$ |

*3.5 IR measurements*

*3.5.1 MZ vibrational modes*

The IR spectra of the free MZ donor and of their corresponding solid CT products were recorded and are shown in Figure 1S. The peak assignments for the important peaks are reported in Table 1S. The free MZ donor shows the following vibrations: *(i) O-H vibrations;* the O-H group gives rise to three vibrations namely stretching, in-plane and out-of plane bending vibrations. Bands due to the O-H stretching are of medium to strong intensity and are generally observed in the region around 3500 $cm^{-1}$. The strong band observed at 3219 $cm^{-1}$ in the IR spectrum of MZ is assigned to O-H stretching vibrations. The O-H in-plane bending vibration appears as a strong band at 1265 $cm^{-1}$, while the O-H out-of-plane deformation vibration was observed at 679 $cm^{-1}$ [32]. *(ii) C-H vibrations;* it is easy to assign the C-H stretching vibration for the MZ donor because it has only one C-H stretching unit in the imidazole ring. The hetero aromatic structure of MZ shows the presence of C-H stretching vibration at 3100 $cm^{-1}$, which is the characteristic region for the ready identification of ν(C–H) [33]. *(iii) $CH_2$ group vibrations;* the C-H stretching vibrations of the methylene group are at lower frequencies than those of the aromatic C-H ring stretching. The asymmetric $CH_2$ stretching vibration is generally observed in the region 3000-2900 $cm^{-1}$, while the $CH_2$ symmetric stretch will appear between 2900-2800 $cm^{-1}$ [34]. The bands observed at 2982 and 2850 $cm^{-1}$ in the IR spectrum of MZ are assigned to $\nu_{as}(CH_2)$ and $\nu_{s}(CH_2)$ modes, respectively. *(iv) $NO_2$ vibrations;* the molecule with $NO_2$ group possesses $\nu_{as}(NO_2)$ band in the range 1625-1540 $cm^{-1}$ and that of the $\nu_{a}(NO_2)$ vibration in the range 1400-1360 $cm^{-1}$ [35]. The bands observed at 1535 and 1369 $cm^{-1}$ are assigned to $\nu_{as}(NO_2)$ and $\nu_{a}(NO_2)$ vibrations, respectively. The deformation vibrations of $NO_2$ group (scissoring, wagging, rocking and twisting) contribute to several normal modes in the low frequency region. The bands observed at 826 and 744 $cm^{-1}$ are assigned to $NO_2$ scissoring and wagging modes, respectively. *(v) Methyl group vibrations;* MZ donor possesses one $CH_3$ group. The bands observed at 3017 and 2956 $cm^{-1}$ are assigned to $\nu_{as}(CH_3)$ and $\nu_{s}(CH_3)$ modes, respectively, while the bands observed at 1429 and 949 $cm^{-1}$ are

ACCEPTED MANUSCRIPT

assigned to $CH_3$ deformation and rocking vibrations, respectively. The rocking vibrations of $CH_3$ group unit appear as independent vibrations. *(vi) Ring vibrations (C-N, C=N vibrations);* the band observed at 1486 $cm^{-1}$ as a very strong band is assigned to the C=N stretching mode. The bands at 1265 and 1074 $cm^{-1}$ are assigned to $\nu_{as}$(C-N) (overlapping with the O-H in-plane bending band) and $\nu_a$(C-N) vibrations, respectively.

*3.5.2 Complexes vibrational modes*

*(i) Iodine complex*

The stretching vibrational of ν(C=N) absorption band of free MZ donor is appeared at 1486 $cm^{-1}$ and under complexation this band was shifted and exhibited decreased intensity. The bands of ν(O-H), $\nu_s$(C-N), $\nu_{as}$(C-N) and δ(C-N) were still unshifted. The observed shift in the ν(C=N) band upon complexation clearly indicated that the –C=N moiety of the donor participated in the CT bonding with iodine. Furthermore, the nitro vibration bands; $\nu_{as}(NO_2)$, $\nu_{as}(NO_2)$ and $\delta(NO_2)$, slightly shifted with respect to those of the free donor; this is most likely due to intermolecular CT interactions. Such shifts suggest electron transfer from the N atom of the donor to the iodine molecule to form the corresponding triiodide complex. The observed UV-vis spectrum of this system confirmed the formation of the $[MZ–I]^+I_3^-$ complex. The IR measurements indicate that the electron transfer from the N atom of (C=N) group in the imidazole ring not from the N atom of (C-N) group. The nitrogen atom of (C=N) is a π-deficient nitrogen which is more basic rather than the π-excessive nitrogen of (C-N). The lone pair of electrons of π-deficient N atom presents in a polarized-hybridized $sp^2$ orbital, but in the π-excessive N atom it present in a non-hybridized *p* orbital (Scheme 3). Furthermore, the presence of the $NO_2$ group in the imidazole ring decreases the electronegativity of the π-deficient N atom (*ortho* position) while, it has no effect towards the π-deficient N atom (*meta* position).

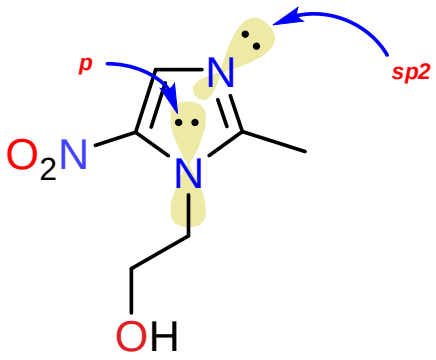


**Scheme 3.** The hybridized and non-hybridized orbitals of the nitrogen atoms in the imidazole ring.

ACCEPTED MANUSCRIPT

Raman spectroscopy can provide valuable information on the nature and structural features of polyiodide anions. Figure 4 shows the representative Raman spectrum of the MZ–$I_2$ complex. The spectrum of this complex contained the characteristic bands for triiodide ($I_3^-$) at 175, 138 and 87 $cm^{-1}$, corresponding to $\nu_{as}$(I–I), $\nu_s$(I–I) and $\delta(I_3^-)$, respectively. The observed Raman spectrum confirmed the formation of the antisymmetric triiodide ion ($I_3^-$). So, the prepared CT complex could be represented as $[MZ–I]^+I_3$. A general mechanism can be proposed for the formation of the $[MZ–I]^+I_3^-$ complex as follows [36-39]: the dye initially forms an outer complex with iodine in a fast step, followed by its transformation into an inner complex, followed by a fast reaction of the resulting inner complex with another mole of iodine to form a triiodide ($I_3^-$) ion, as depicted below.

| | | |
|---|---|---|
| $MZ + I_2 \leftrightarrows MZ–I_2$ | (outer complex) | Fast |
| $MZ–I_2 \leftrightarrows [MZ–I]^+I^-$ | (inner complex) | Slow |
| $[MZ–I]^+I^- + I_2 \leftrightarrows [MZ–I]^+I_3^-$ | (triiodide complex) | Fast |

*(ii) DDQ complex*

When DDQ acceptor complexed with the MZ donor, the bands that results from the ν(C≡N) vibration of the free DDQ acceptor were changed in frequencies and decrease in intensities upon CT compexation. Free DDQ shows two ν(C≡N) vibration at 2250 and 2331 $cm^{-1}$, while in its complex it occur at 2235 and 2211 $cm^{-1}$. The cyano group (C≡N) is an electron-withdrawing group that exists in DDQ in a conjugated bonding system. The CN groups in DDQ withdraw electrons from the aromatic ring, and such a process will make the aromatic ring an electron-accepting region. Instead, MZ donor contains high electron density over the imidazole ring (five π electrons over 6 atoms in the ring). Only the fully saturated nitrogen atom of (C-N) group is in a position to donate its lone pair of electrons into the π-system and contributes in the aromaticity of the imidazole ring. So, because of the electron-withdrawing process and the conjugated electron system in the DDQ acceptor, and the good electron-donating ability of the imidazole ring, the interactions mode (MZ→DDQ) occur through π→π* charge migration via the imidazole ring of the MZ donor and the aromatic ring of the DDQ acceptor [40-45].

*(iii) CHL complex*

When CHL acceptor complexed with the MZ donor, the vibration frequency of the ν(C=N) and ν(O-H) for MZ existed at 1486 and 3219 $cm^{-1}$, respectively, were still unshifted, this meaning that C=N and O-H groups are not participated in the CT complezation. The group of bands observed at 3093, 2951, 2843 $cm^{-1}$ in this complex were assigned to $\nu_s$(C-H) + $\nu_{as}$(C-H) vibrations with different position wavenumbers compared with the free MZ. The stretching vibrational of ν(C=O) absorption band of free CHL is appeared at 1685 $cm^{-1}$ and under complexation this band was still unshifted. The bands associated with ν(C-Cl) at 903 and 709 $cm^{-1}$ in the free CHL were shifted to lower wavenumbers and decreasing in the intensities of the characteristic peaks, these shifts due to the increasing in the electron density around CHL moiety. The interactions mode (MZ→CHL) can be occur through π→π* transition.

ACCEPTED MANUSCRIPT

*(iv) PA complex*

When PA acceptor was complexed with the MZ donor, the characteristic bands of the free donor and acceptor were shifted and decreased in the intensities. The outlined changes in the bands of ν(C=N) (for MZ donor) and ν(O–H) (for PA acceptor) upon complexation clearly supports the formation of the CT complexes between donor and acceptor. The vibrational absorption band of ν(O–H) was shifted to higher frequencies while those of ν(C=N) was shifted to lower frequencies. This complex is also characterized by a medium bands appearing in the region between 2400 and 2800 $cm^{-1}$. These broadened bands presence at 2742, 2567, 2496 $cm^{-1}$ was attributed to the stretching vibration of a proton attached to the donation site (C=N) of the donor and forming $^{+}$NH group. All these observations indicates that the complexation occurs through the formation of intermolecular H-bonding between the basic center on the donor (C=N group) and the acidic center on the acceptor (OH group) [46-52].

*3.6 $^{1}$H NMR measurements*

The nuclear magnetic resonance, 400 MHz $^{1}$H NMR spectrum of the complex containing the PA acceptor was measured in DMSO-$d_6$ solvent at room temperature using tetramethylsilane (TMS) as internal standard. The positions of chemical shift (δ) of the different types of protons are expected to be shifted based on the changes in the electronic environment around the protons attached to the groups which contain the site of donation and involvement in the complexation. The free MZ donor produced signals at δ = 2.37 (s, 3H, $CH_3$), 3.76 (t, 2H, $CH_2$, $CH_2C\underline{H}_2OH$), 4.35 (t, 2H, $CH_2$, $C\underline{H}_2CH_2OH$), 4.64 (t, 1H, OH), 7.91 (s, 1H, imidazole proton) [33]. The reaction of MZ donor with PA acceptor yielded a new CT complex, which produced signals at (Figure 5) δ = 2.60 (s, 3H, $CH_3$), 3.74 (t, 2H, $CH_2$, $CH_2C\underline{H}_2OH$), 4.47 (t, 2H, $CH_2$, $C\underline{H}_2CH_2OH$), 7.45 (s, 3H, OH proton and 2 H for picric acid protons), 8.49 (s, 1H, imidazole proton), 8.59 (s, 1H, $^{+}$NH, hydrogen bonded with picric acid OH). Free MZ donor displays characteristic signal at 4.64 ppm, corresponding to the (–OH) proton. On complexation with PA and acceptor, this signal was shifted and appeared at new δ values at δ =7.45 ppm. The peak at δ =11.94 ppm, which is assigned to the (–OH) proton of free picric acid [53], is absence in the spectrum of this complex. Instead, the peak appeared at 8.59 ppm, is assigned to $^{+}$NH proton. It is clearly obvious that the formation of this new signal indicating the involvement of the imine nitrogen of donor and (–OH) group of acceptor in chelating through the deprotonation from the PA to the MZ. The intensities and chemical shifts of the aromatic signals were significantly affected by the existence of the ($N^{+}$—H) charge-transfer interaction between the donor and the acceptor molecules. The downfield shift for the imidazole ring proton may be attributed to the presence of the electron deficient PA ring which resulted in a deshielding to the entire imidazole ring and its substituents protons.

*3.7 Complexation pathway*

The results of elemental analyses, UV-vis, IR and $^{1}$H NMR spectral data are in agreement with each other to support the predicted structures of the obtained CT complexes. The suggested complexation mechanism of the CT complexes between MZ donor with different acceptors is illustrated in Scheme 4.

ACCEPTED MANUSCRIPT

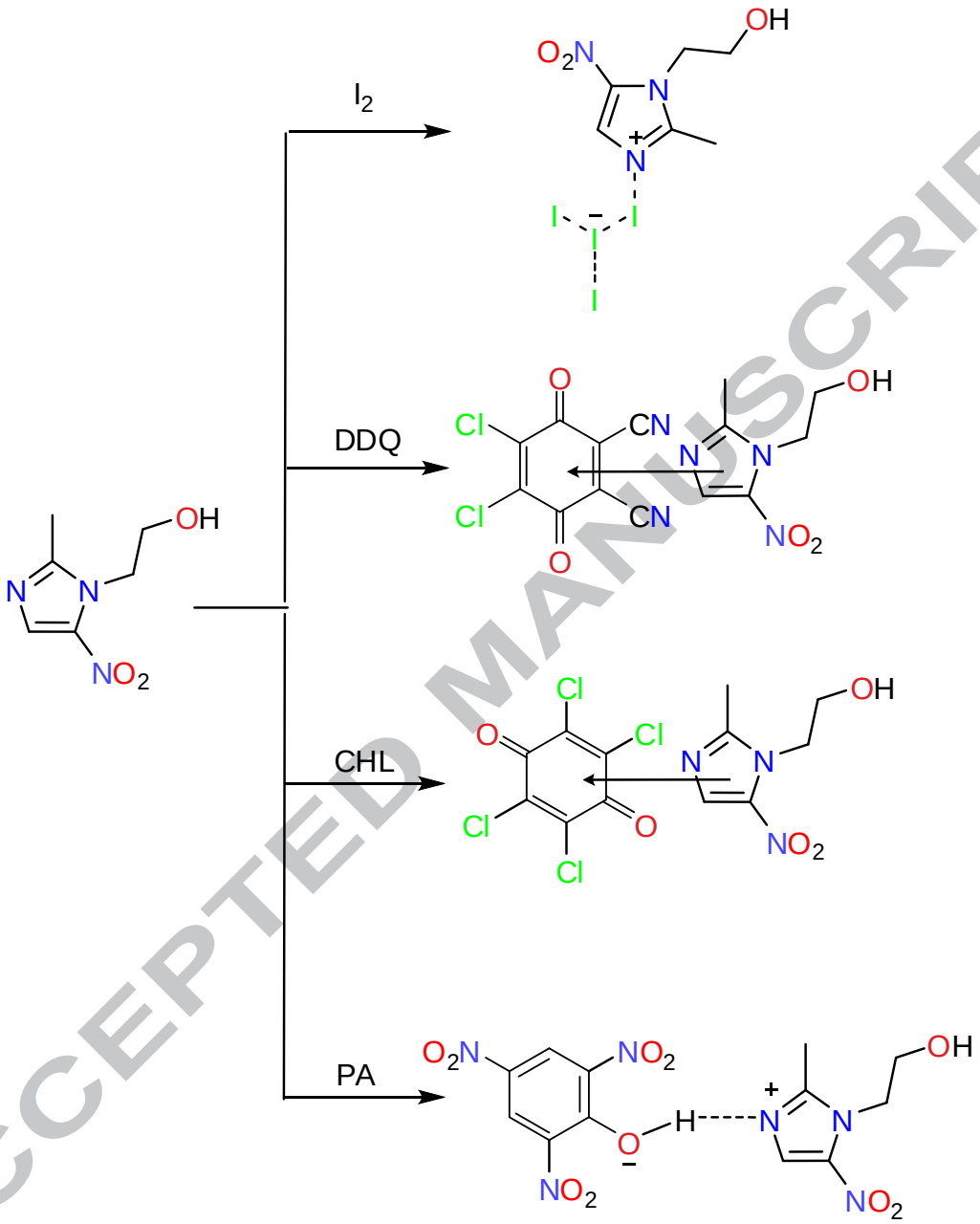


**Scheme 4.** Proposed structural formula of the MZ CT complexes.

ACCEPTED MANUSCRIPT

*3.8 TG and DTG profiles*

To confirm the composition and structures of the formed solid CT complexes, Thermal analyses (TG and DTG) were carried out for the MZ donor and its complexes with $I_2$, DDQ, CHL and PA acceptors. The measurements were carried out under nitrogen atmosphere in the temperature range of 25-800 °C. Their representative thermograms are illustrated in Figure 2S. The possible thermal degradation patterns for these compounds are collected in Table 2S. Fairly close values of the calculated and experimental percentage of the moieties expelled from these complexes strongly support the experimentally determined stoichiometry of the complexes.

The TG and DTG thermogram of the MZ donor indicated that this drug is thermally stable in the 25-145 °C temperature range. The thermal decomposition of the drug proceeds via one degradation step, corresponding to a very strong endothermic peak at 244 °C. The donor begins decomposed at ~145 °C and was complete at ~500° C, and the observed weight loss associated with this step is (obs.=99.91, cal.= 100.0%), which can be attributed to the loss of the $C_6H_9N_3O$ organic moiety ($2.5C_2H_2+NO_2+N_2+CO+2H_2$). The complex containing the iodine acceptor was thermally decomposed in nearly two decomposition steps within the 80-600 °C temperature range. The first mass loss (obs.=62.57, cal.= 62.61%) with $DTG_{max}$ of 212 °C corresponds to the libration of MZ and one $I_2$ molecule. The second decomposition step at maximum ~270 °C founded within the 350-600 °C temperature range (obs.=36.80, cal.= 37.39%) which may be assigned to the removal of one $I_2$ molecule. Figure 2S (c) shows the thermogram of the [(MZ)(DDQ)] complex. It decomposes in three degradation steps; at temperature ($DTG_{max}$) 67, 225 and 688 °C. The first decomposition step in the temperature range of 50-270 °C has a weight loss of approximately 31.36% and is attributed to the loss of 2HCN and $CL_2$ moieties. The second decomposition step occurred within the 270-550 °C temperature range and was assigned to the removal of $C_2H_2+NO_2+NO+2.5H_2$ molecules. The final decomposition step occurred within the 550-800 °C temperature range corresponding to loss of $NO_2$ representing a weight loss of (obs.=10.76, cal.= 11.56%) then leaving residual carbon as final products. Figure 2S (d) shows the thermal behavior of the [(MZ)(CHL)] complex. From the first step 120-260 °C, the mass loss at $DTG_{max}$ of 198 is (obs.=58.91, cal.= 58.96%) which is reasonably by the loss of CHL moiety. Continuous mass loss in the TG curve from 260-750 °C corresponds to the loss of the donor moiety (obs.=40.89, cal.= 41.04%). The thermal degradation of the [(MZ)(PA)] complex occurs in two degradation stages within the 155-800 °C temperature range. These stages are correspond to a single strong and sharp endothermic peak at 245 °C, and are associated with weight losses of 71.9% and 13%. The first stage of decomposition corresponds to the loss of $4NO_2+C_2H_2+CO_2+N_2+3H_2$ molecules with a weight loss of 71.9%, which is in good agreement with the calculated value (71.96%). The second stage of decomposition corresponds to the loss of two $C_2H_2$ molecules with a weight loss of 13.02% very close to the expected theoretical value of 12.99%. The final decomposition of the complex is the residual carbon atoms.

ACCEPTED MANUSCRIPT

*3.9 Kinetic-thermodynamic data*

The Kinetic-thermodynamic parameters (i.e., the activation energy ($E^*$), the frequency factor ($A$), the enthalpy of activation ($H^*$), the entropy of activation ($S^*$) and the Gibbs free energy of activation ($G^*$)) associated with the MZ donor and its CT complexes were evaluated graphically (Figure 3S) by employing the Coats–Redfern and Horowitz–Metzger methods, previously described in section (2.4.2), and the evaluated data are listed in Table 3S. The kinetic-thermodynamic data obtained from the two methods are comparable and can be considered in good agreement with each other. The activation energy ($E^*$) of the complexes is expected to increase with the increasing thermal stability of complexes. Therefore, the $E^*$ value for the [(MZ)(CHL)] complex is higher compared to the other complexes, which indicates the higher thermal stability of the [(MZ)(CHL)] complex. By comparing the $E^*$ values for the main decomposition stage of the complexes, we observed the following trend for the different acceptors: CHL > PA > DDQ > Iodine. These differences may be due to the reactivity of the complexes and the electronic configuration of the acceptor when complexed with the MZ donor. The negative values of the $\Delta S^*$ indicate that the activation complexes have more ordered structure than the reactants. The $\Delta S^*$ values of the complexes occur in a decreasing order for the different acceptors as follows: CHL > PA > Iodine > DDQ. A liner relationship obtained between $\Delta H^*$ and $\Delta S^*$ (Figure 6) for all complexes. It has been found that the complexation with CHL and PA acceptors increases the values of enthalpy and entropy, while the complexation with DDQ and iodine acceptors decreases the values of these parameters compared with the free MZ donor.

## 4. Conclusions

As one of the important nitroimidazole derivatives, metronidazole (MZ) has been widely used as antimicrobial medicine. Herein this work, physico-chemical and thermal characteristics of MZ complexes with iodine, DDQ, CHL and PA were reported. MZ reacts instantly with the reported acceptors to form colored CT complexes. Significant changes in the ultraviolet-visible spectra were observed and may be attributed to the formation of the CT complexes. Elemental analyses and spectrophotometric titration methods conclude that the complexes are formed based on a 1:1 stoichiometric ratio, except for iodine acceptor (1:2 ratio). The isolated solid complexes were structurally and thermally characterized using UV-vis, IR, $^1$H NMR and thermal techniques. TG analysis indicates that the formation of the complexes was stable, exothermic and spontaneous. Our study provides a basis to understand the mechanism of the interaction of drug MZ with different σ- and π-acceptors

ACCEPTED MANUSCRIPT

**References**

[1] I.M. Khan, A. Ahmad, M.F. Ullah, J. Photochem. Photobio. B 103 (2011) 42.
[2] I.M. Khan, A. Ahmad, M.F. Ullah, Spectrochim. Acta A 102 (2013) 82.
[3] I.M. Khan, A. Ahmad, M. Aatif, J. Photochem. Photobio. B 105 (2011) 6.
[4] I.M. Khan, A. Ahmad, J. Mol. Struct. 975 (2010) 381.
[5] I.M. Khan, A. Ahmad, J. Mol. Struct. 977 (2010) 189.
[6] I.M. Khan, A. Ahmad, S. Kumar, J. Mol. Struct. 1035 (2013) 38.
[7] M. Saravanabhavan, K. Sathya, V.G. Puranik, M. Sekar, Spectrochim. Acta A 118 (2014) 399.
[8] H.H. Eldaroti, S.A. Gadir, M.S. Refat, A.M.A. Adam, Spectrochim. Acta A 115 (2013) 309.
[9] H.H. Eldaroti, S.A. Gadir, M.S. Refat, A.M.A. Adam, Spectrochim. Acta A 109 (2013) 259.
[10] H.H. Eldaroti, S.A. Gadir, M.S. Refat, A.M.A. Adam, J. Pharm. Anal. 4 (2) (2014) 81.
[11] Beena, N. Kumar, R.K. Rohilla, N. Roy, D.S. Rawat, Bioorg. Med. Chem. Lett. 19 (2009) 1396.
[12] X.J. Huang, J.B. Lin, D.X. Yuan, J. Sep. Sci 34 (2011) 2138.
[13] D. Chen, J. Deng, J. Liang, J. Xie, C. Hu, K. Huang, Sensors Actuators B 183 (2014) 594.
[14] T. Chen, L. Chen, H. Li, Y. Chen, H. Guo, Y. Shu, Z. Chen, C. Cai, L. Guo, X. Zhang, L. Zhou, Q. Zhong, Colloides Surfaces B: Biointerfaces 118 (2014) 65.
[15] L. Fu, X-f Liu, Q-x Zhou, J-x Zhang, J-y Dong, J-f Wang, J. Luminescence 149 (2014) 208.
[16] A. Sadowska, S. Prokopiuk, W. Miltyk, A. Surażyński, J. Konończuk, D. Sawicka, H. Car, Advances in Medical Sciences 58 (1) (2013) 90.
[17] D.S. Lindsay, B.L. Blagburn, Veterinary pharmacology and therapeutics, in: H.R. Adams (Ed.), Antiprotozoan Drugs, Iowa State University Press, Ames, 2001, pp. 992-1016.
[18] C.M. Santana, Z.S. Ferrera, M.E.T. Padrón, J.J.S. Rodríguez, Anal. Chim. Acta 665 (2010) 113.
[19] M.E. Falagas, A.M. Walker, H. Jick, R. Ruthazer, J. Griffith, D.R. Snydman, Clin. Infect. Dis. 26 (2) (1998) 384.
[20] M.J. Kasten, Mayo Clin. Proc. 74 (8) (1999) 825.
[21] H.A. Benesi, J.H. Hildebrand, J. Am. Chem. Soc. 71 (1949) 2703.
[22] R. Abu-Eittah, F. Al-Sugeir, Can. J. Chem. 54 (1976) 3705-3712.
[23] G. Briegleb, Z. Angew. Chem. 76 (1964) 326.
[24] H. Tsubomura, R.P. Lang, J. Am. Chem. Soc. 83 (1961) 2085.
[25] R. Rathore, S.V. Lindeman, J.K. Kochi, J. Am. Chem. Soc. 119 (1997) 9393.
[26 ] G.G. Aloisi, Pignataro, J. Chem. Soc. Faraday Trans. 69 (1973) 534-539.
[27] A.W. Coats, J.P. Redfern, Nature (London) 201 (1964) 68.
[28] H.H. Horowitz, G. Metzger, Analytical Chemistry 35 (1963) 1464.
[29] W. Kiefer, H.J. Bernstein, Chem. Phys. Lett. 16 (1972) 5.
[30] L. Andrews, E.S. Prochaska, A. Loewenschuss, Inorg. Chem. 19 (1980) 463.
[31] K. Kaya, N. Mikami, Y. Udagawa, M. Ito, Chem. Phys. Lett. 16 (1972) 151.
[32] G. Varsanyi, Assignments for Vibrational Spectra of Seven Hundred Benzene Derivatives, Vol. 1 and 2, Academic Kiado: Budapest, 1973.
[33] S.P.V. Chamundeeswari, E.R.J.J. Samuel, N Sundaraganesan, Eur. J. Chem. 2 (2) (2011) 136.

ACCEPTED MANUSCRIPT

[34] D. Sajan, J. Binoy, B. Pradeep, K.V. Krishnan, V.B. Kartha, I.H. Joe, V.S. Jayakumar, Spectrochim. Acta A 60 (2004) 173.
[35] B. Lakshmaiah, G. Rao Ramana, J. Raman Spectrosc. 20 (1989) 439.
[36] M. Pandeeswaran, K.P. Elango, Spectrochim. Acta A 72 (2009) 789.
[37] M. Pandeeswaran, K.P. Elango, J. Sol. Chem. 38 (12) (2009) 1558.
[38] K. Ganesh, C. Balraj, K.P. Elango, Spectrochim. Acta A 79 (2011) 1621.
[39] K. Ganesh, K.P. Elango, Spectrochim. Acta A 93 (2012) 185.
[40] M.S. Refat, O.B. Ibrahim, H.A. Saad, A.M.A. Adam , J. Mol. Strut. 1064 (2014) 58.
[41] M.S. Refat, M.Y. El-Sayed, A.M.A. Adam, Can. Chem. Trans. 2 (2014) 149.
[42] H.H. Eldaroti, S.A. Gadir, M.S. Refat, A.M.A. Adam, Int. J. Electrochem. Sci. 8 (2013) 5774.
[43] A.M.A. Adam, J. Mol. Struct. 1030 (2012) 26.
[44] G.G. Mohamed, S.M. Khalil, M.A. Zayed, M. A. El-Shall, J. Pharm. Biomed. Analysis 28 (2002) 1127.
[45] A.S. Amin, M.E. Moustafa, Y.M. Issa, Microchem. J. 50 (1994) 6.
[46] N. Singh, I.M. Khan, A. Ahmad, S. Javed, J. Mol. Liquids 191 (2014) 142.
[47] A.A. El-Habeeb, F.A. Al-Saif, M.S. Refat, Spectrochim. Acta A 123 (2014) 455.
[48] M.S. Refat, A.M.A. Adam, T. Sharshar, H.A. Saad , H.H. Eldaroti, Spectrochim. Acta A 122 (2014) 34.
[49] A.M.A. Adam, M.S. Refat, H.A. Saad, J. Mol. Strut. 1051 (2013) 144.
[50] A.M.A. Adam, M.S. Refat, H.A. Saad, J. Mol. Strut. 1037 (2013) 376.
[51] A.M.A. Adam, Spectrochim. Acta A 104 (2013) 1.
[52] I.M. Khan, A. Ahmad, J. Mol. Struct. 1050 (2013) 122.
[53] R.D. Kross, V.A. Fassel, J. Am. Chem. Soc. 79 (1957) 38.

ACCEPTED MANUSCRIPT

ACCEPTED MANUSCRIPT

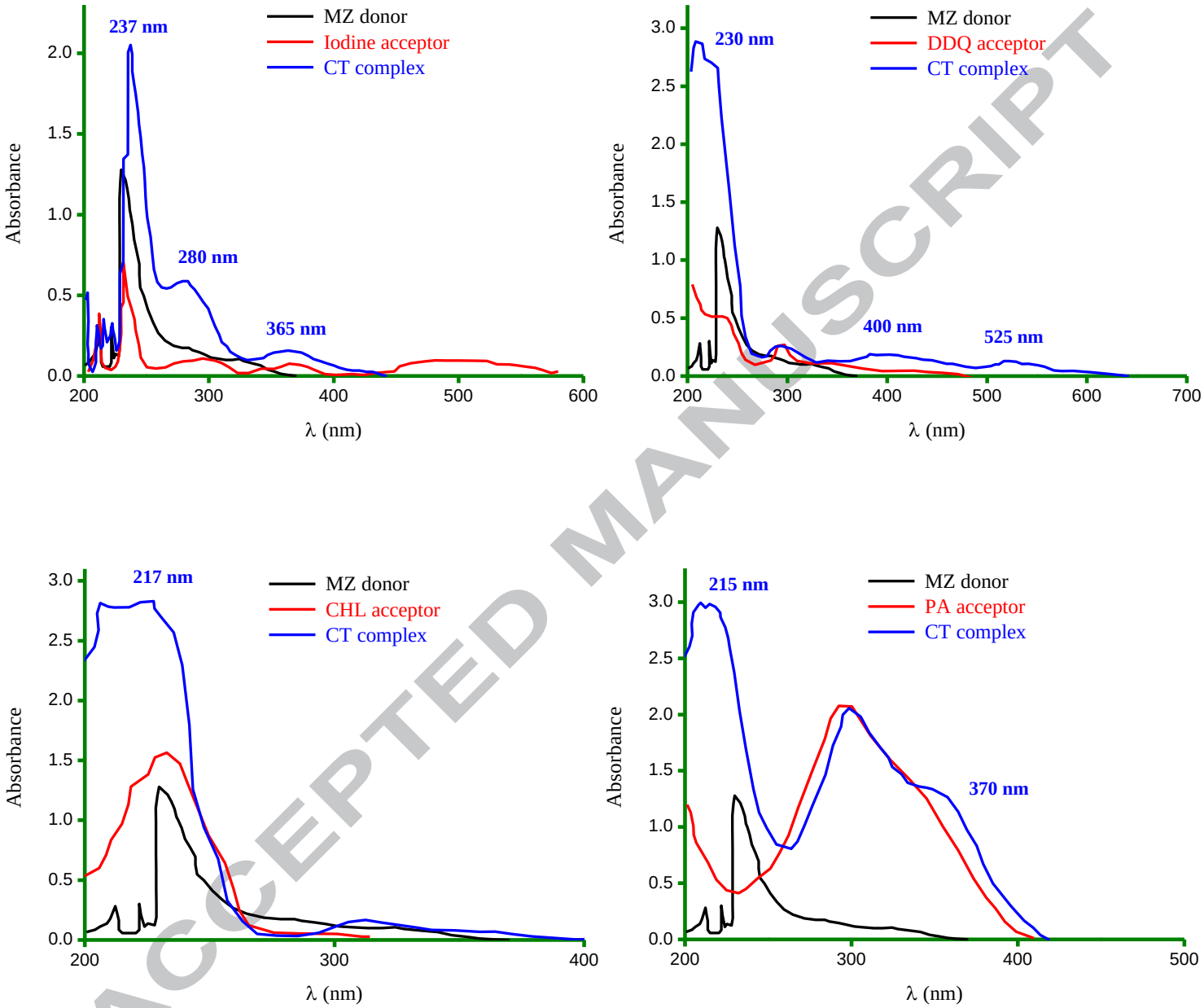


**Figure. 1:** Electronic spectra of MZ–$I_2$, MZ–DDQ, MZ–CHL and MZ–PA complex.

ACCEPTED MANUSCRIPT

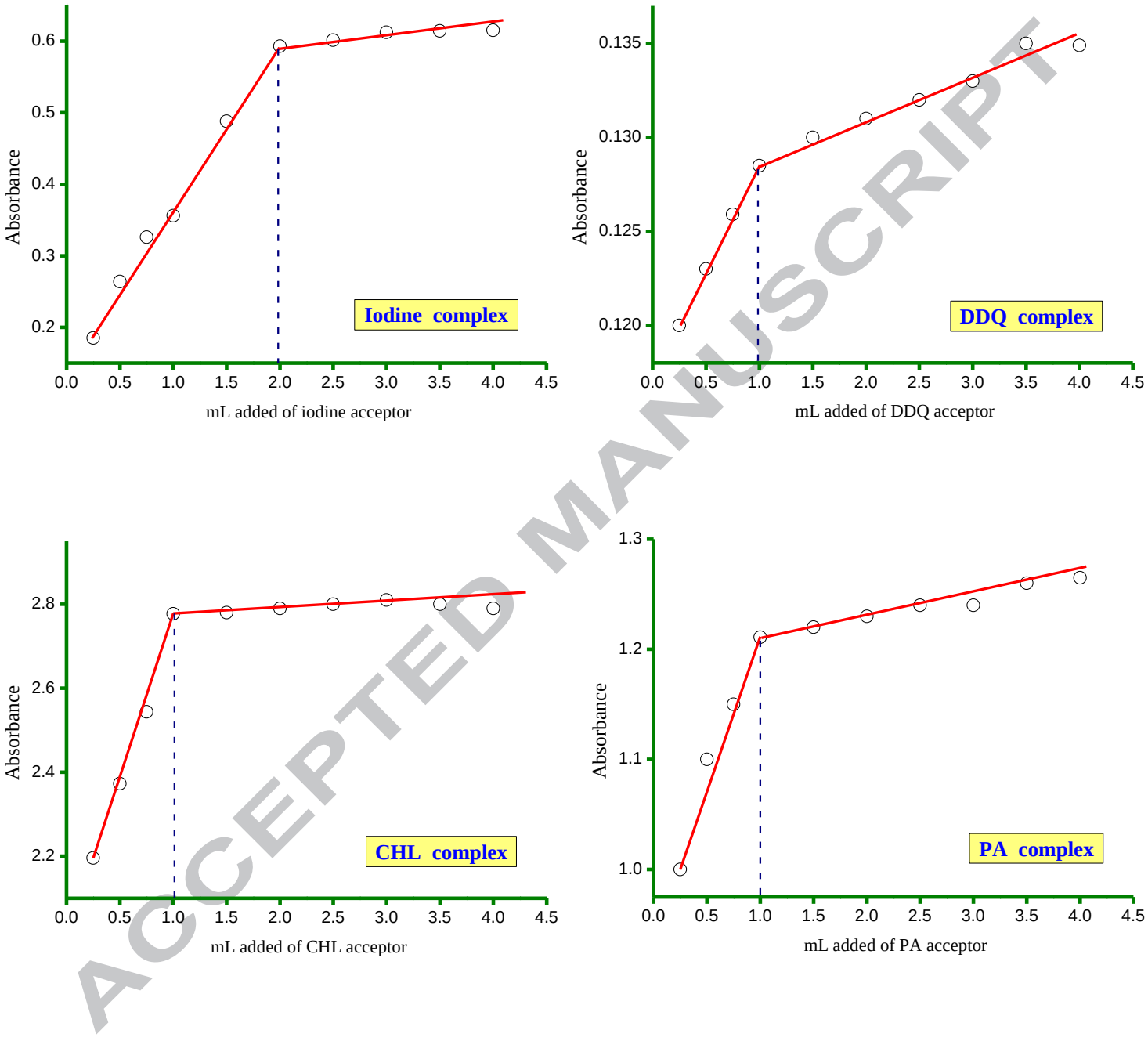


**Figure 2.** Spectrophotometric titration curves for MZ–$I_2$, MZ–DDQ, MZ–CHL and MZ–PA systems.

ACCEPTED MANUSCRIPT

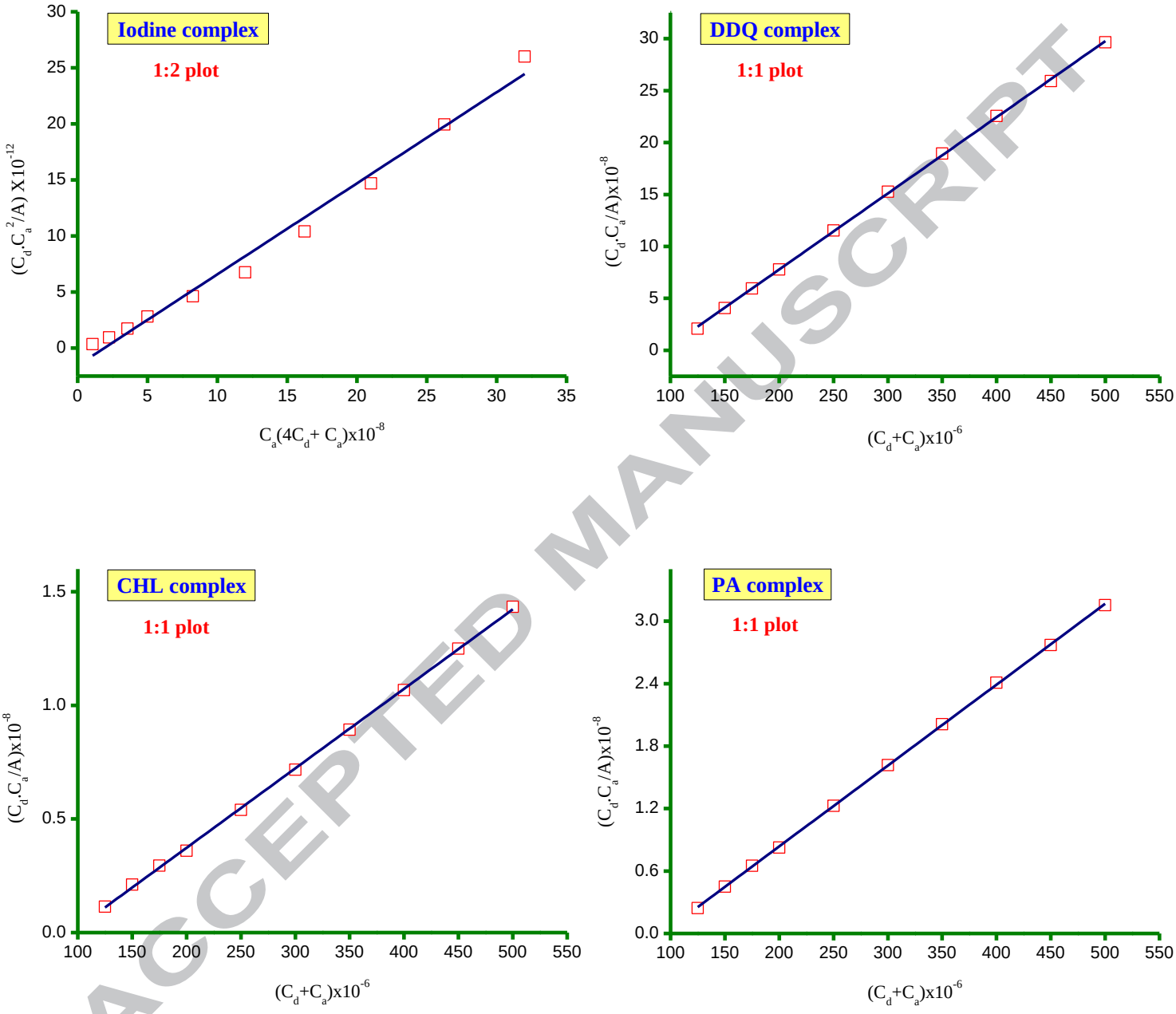


**Figure 3**. The 1:1 and 1:2 Benesi–Hildebrand plots for MZ–$I_2$, MZ–DDQ, MZ–CHL and MZ–PA systems.

ACCEPTED MANUSCRIPT

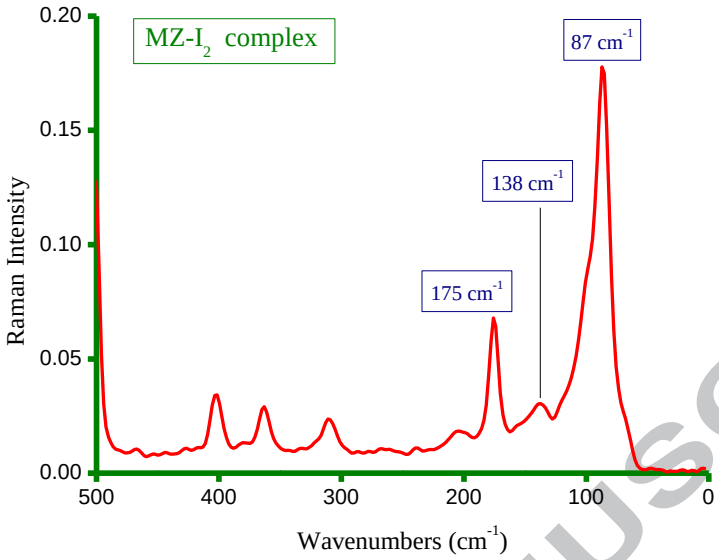


**Figure 4.** Raman spectrum of MZ–Iodine complex.

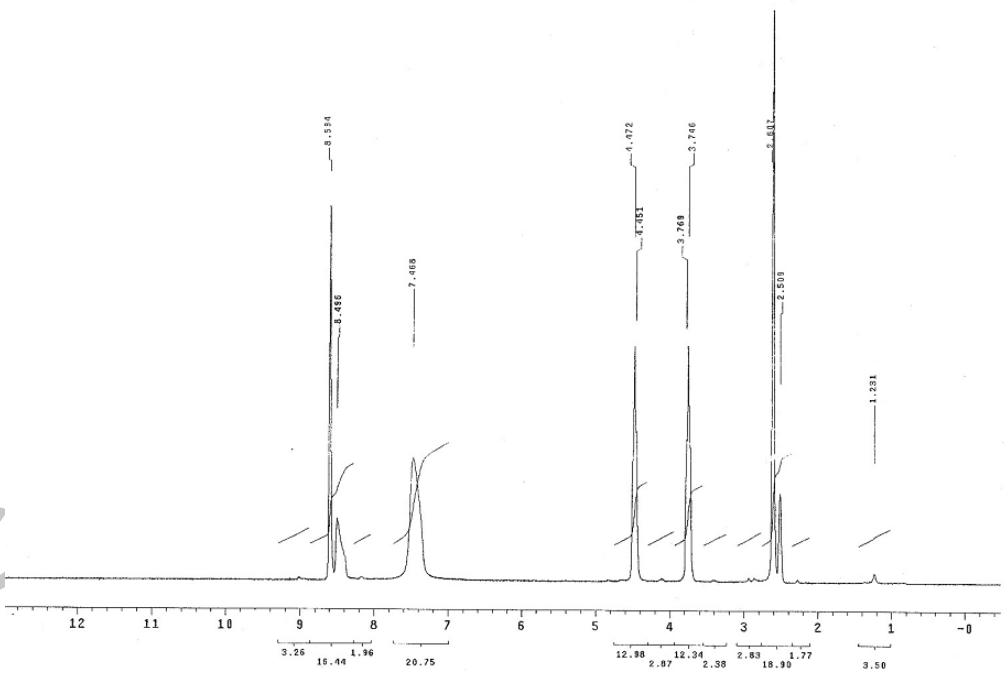

**Figure 5.** $^{1}$H NMR spectrum of MZ–PA complex.

ACCEPTED MANUSCRIPT

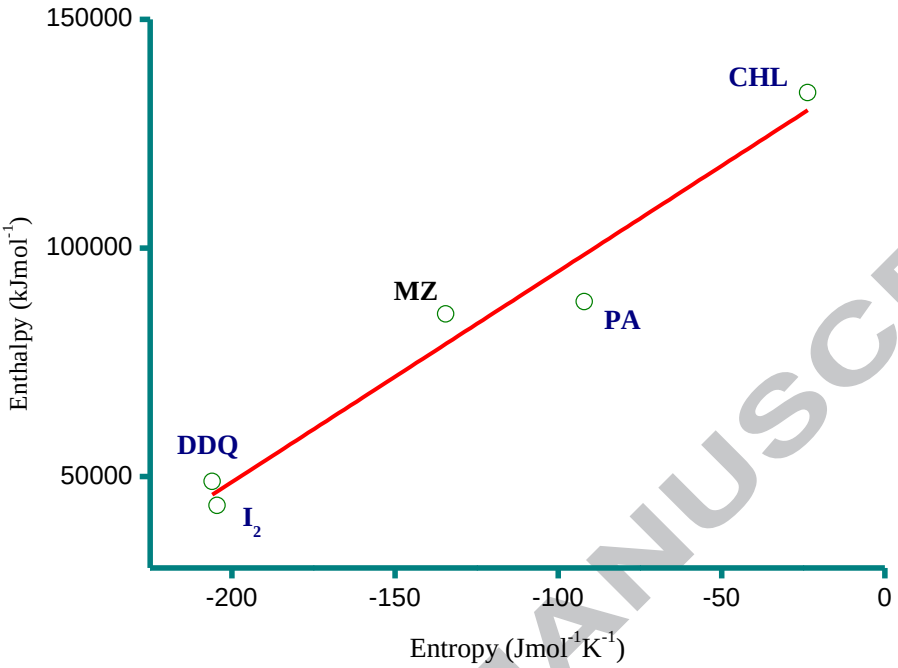


**Figure 6.** Linear correlation between enthalpy and entropy of the MZ complexes.

ACCEPTED MANUSCRIPT

ACCEPTED MANUSCRIPT

**Graphical Abstract**

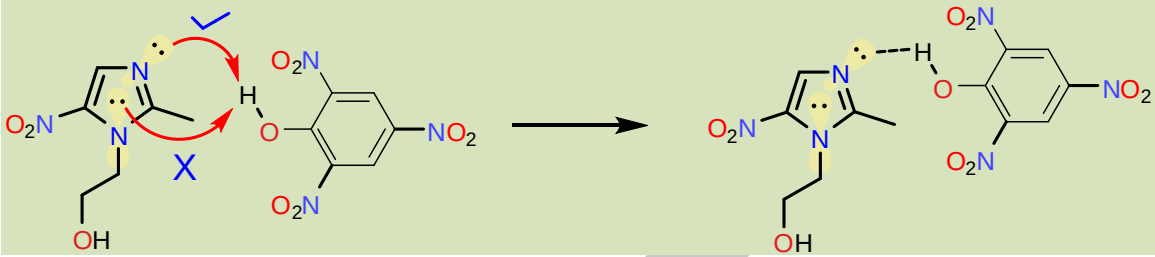


The complexation chemistry of drug metronidazole with picric acid

ACCEPTED MANUSCRIPT

ACCEPTED MANUSCRIPT

**Highlights**

- Complexation chemistry of drug metronidazole with different acceptors was studied.
- The interactions were characterized both in solution and in the solid state.
- Spectroscopic, thermal and kinetic properties were determined.

ACCEPTED MANUSCRIPT